1

Introduction

1.1 INTRODUCTION

Mankind has exploited matter in technology through the ages. For many millenia, we relied on materials like wood or metals that were subject to minimal processing to provide useful objects. It is only within a few minutes of midnight on the proverbial human evolutionary clock that materials have been engineered for ultimate applications based on a deep understanding of molecular properties. Considering substances that have been engineered in a controlled or tailored manner, the nineteenth century was the age of iron and steel. The twentieth century saw the development of new types of engineered materials, especially polymers, which in the form of plastics have, in many applications, usurped many of the traditional 'hard' materials. This is not to forget the emergence of an important class of inorganic material, semiconductors, in the second half of this century. These are, of course, the basis for the second industrial revolution, that of information technology. However, it seems fair to say that many properties of hard matter are now well understood whereas we are still on the learning curve with soft matter. For example, inspired by nature, we are only just beginning to be able to engineer complex structures formed by biopolymers or to exploit nanotechnology to make devices based on self-organization of polymers. In our new millennium it seems safe to predict the continued importance of soft materials, engineered in ways we can as yet only dream of.

The idea of a unified approach to 'soft materials' has only gained ground recently. It is an interdisciplinary subject, taking in aspects of physics, chemistry and materials science, but also of biochemistry or (chemical, mechanical) engineering in specific cases. A consequence of this

Introduction to Soft Matter – Revised Edition: Synthetic and Biological Self-Assembling Materials I. W. Hamley

interdisciplinarity is that, unfortunately, the subject is not considered in conventional textbooks on physics, physical chemistry or materials science, often being neglected entirely or covered in an inadequate manner. The purpose of this book is to 'fill the gap', by providing an up-to-date introductory summary of the thermodynamics and dynamics of soft materials. In each of the six chapters, the basic physical chemistry is covered first, prior to an outline of applications. The material is presented in a coherent fashion across the book. Equations have been kept to the minimum number that capture important relationships. Derivations are included, where they illustrate thermodynamical or statistical mechanical principles in action. The derivation of the Flory–Huggins theory in Section 2.5.6 or of the thermodynamics of micellar equilibria in Section 4.6.5 are good examples. Soft materials are important in many products, such as detergents, paints, plastics, personal care products, foods, clays, plastics and gels. Such uses of soft materials are exemplified throughout this book.

In this book we consider soft materials under the headings of polymers (Chapter 2), colloids (Chapter 3), amphiphiles (Chapter 4), liquid crystals (Chapter 5) and biological soft materials (Chapter 6). The distinctions between these systems are often not strong. For example, amphiphiles in solution and some aspects of polymer science are often considered in books on colloid chemistry. However, here we treat them separately since they are technologically important enough to merit detailed consideration on their own. The chapter on liquid crystals is in fact focused on one class of material, thermotropic liquid crystals, where phase transitions are thermally driven. However, a different class of liquid crystal phase is formed in amphiphile solutions, where concentration is also a relevant variable. These are termed lyotropic liquid crystal phases and are discussed in Chapter 4.

There are a number of texts that deal with aspects of the subjects covered in this book. General texts in the area include those by Evans and Wennerström, Hunter, Larson and Shaw (see Further Reading at the end of the chapter). Detailed textbooks for background reading on each topic are listed in the Further Reading section that follows each chapter. In Chapter 2, polymer science is outlined in a particularly concise form, and after the fundamentals are introduced, attention is paid to applications of polymers in the latter part of the chapter. There are quite a number of monographs concerned with colloids. However, many of these are not suitable for use as undergraduate textbooks. Thus, Chapter 3 fulfills a particularly useful function in providing an up-to-date introduction to the essential physical chemistry. Also emphasized are applications of colloids and colloids in everyday life, such as in foods. Chapter 4 summarizes the important aspects underpinning the self-assembly of amphiphiles, i.e. surfactants and lipids. The action of surfactants as detergents is also considered and the importance of lipids in cell membranes is discussed. Chapter 5 is concerned with thermotropic liquid crystals. Chapter 6 is focused on aspects of self-assembly of biological soft materials. Recommended texts for background reading on these subjects are listed in the Further Reading sections.

In this chapter, intermolecular forces that are the basis of self-assembly are considered in Section 1.2. Section 1.3 outlines common features of structural ordering in soft materials. Section 1.4 deals similarly with general considerations concerning the dynamics of macromolecules and colloids. Section 1.5 focuses on phase transitions along with theories that describe them, and the associated definition of a suitable order parameter is introduced in Section 1.6. Scaling laws are defined in Section 1.7. Polydispersity in particle size is an important characteristic of soft materials and is described in Section 1.8. Section 1.9 details the primary experimental tools for studying soft matter and Section 1.10 summarizes the essential features of appropriate computer simulation methods.

1.2 INTERMOLECULAR INTERACTIONS

The term 'soft' matter originates from macroscopic mechanical properties. We mean here materials such as colloids, surfactants, liquid crystals, certain biomaterials and polymers in the melt or solution. Many soft materials can be induced to flow under certain conditions. This weak ordering results from the lack of three-dimensional atomic long-range order found in a crystalline solid. Nevertheless, there is always a degree of local order at least as great as that in a liquid. From the viewpoint of kinetic energy, a crude distinction between 'soft' materials and 'hard' ones can be made on the basis that the molecular kinetic energy for the former is close to k_BT, whereas for the latter it is much less than k_BT (when the temperature is near ambient). Here we consider the intermolecular forces responsible for the ordering of soft materials. Our purpose is not to provide a detailed description of these forces, since this is dealt with in many physical chemistry textbooks (for example Atkins, 2006). Here we briefly outline the essential results, especially in the context of self-assembly in soft matter, which is the subject of this book.

The forces between molecules are a balance of repulsive interactions at short distances and attractive interactions that predominate over larger length-scales. This is illustrated by the curve of potential energy as a function of intermolecular separation in Fig. 1.1. We will now consider the origin of the repulsive and attractive forces. Then we consider Coulombic forces since ions are present in solution in many colloid and surfactant systems, and in this case interactions between charged species predominate.

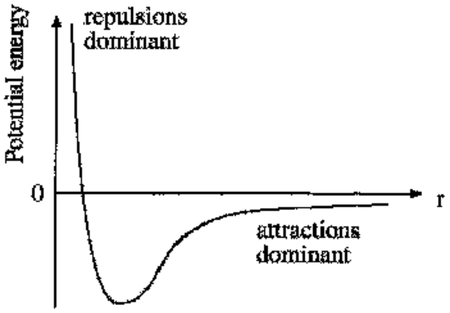

Figure 1.1 Typical curve of potential energy versus separation of two molecules or atoms. At short distances, repulsive interactions predominate, whilst attractive forces act over a longer range

Repulsive interactions are important when molecules are close to each other. They result from the overlap of electrons when atoms approach one another. As molecules move very close to each other the potential energy rises steeply, due partly to repulsive interactions between electrons, but also due to forces with a quantum mechanical origin in the Pauli exclusion principle. Repulsive interactions effectively correspond to steric or excluded volume interactions. Because a molecule cannot come into contact with other molecules, it effectively excludes volume to these other molecules. The simplest model for an excluded volume interaction is the hard sphere model. The hard sphere model has direct application to one class of soft materials, namely sterically stabilized colloidal dispersions. These are described in Section 3.6. It is also used as a reference system for modelling the behaviour of simple fluids. The hard sphere potential, $V(r)$, has a particularly simple form:

$$V(r) = \begin{cases} \infty & \text{for } r \leq d \\ 0 & \text{for } r > d \end{cases} \tag{1.1}$$

where d is the diameter of the hard sphere. The ordering of hard spheres depends only on their volume fraction. The phase diagram has been obtained by computer simulations and experiments on sterically stabilized colloid particles, as discussed in Section 3.6.

The hard sphere model is based on the excluded volume of spherical particles. An excluded volume theory has been developed to account for the orientational ordering of liquid crystal molecules, assuming them to be hard rods. This is the Onsager theory and its variants, outlined in Section 5.5.2. Excluded volume interactions influence the conformation of polymer chains. The conformation of an ideal chain is described by a random walk. However, in this case the chain can cross itself, i.e. it has no excluded volume. Under certain circumstances a polymer chain can behave as if this was the case (see Section 2.3.2). However, it is more usual for excluded volume interactions to lead to a self-avoiding walk, which produces a more extended conformation than that of a random walk (Section 2.3.2).

Because there are no attractive interactions in the potential, the hard sphere model does not describe the forces between molecules very well. More realistic potentials include an attractive contribution, which usually varies as $-1/r^6$ (as discussed shortly) as well as a repulsive term. The latter is chosen to vary as $1/r^n$, with $n > 6$, to ensure that repulsions dominate at short distances, $n = 12$ often being assumed. This combination of attractive and repulsive terms defines the Lennard–Jones (12,6) potential:

$$V(r) = 4\varepsilon\left[\left(\frac{r_0}{r}\right)^{12} - \left(\frac{r_0}{r}\right)^{6}\right] \tag{1.2}$$

Here ε is the depth of the potential energy minimum and $2^{1/6}r_0$ is the intermolecular separation corresponding to this minimum. This potential has a form similar to that shown in Fig. 1.1. It is often used as a starting point for modelling intermolecular interactions, for example it can be chosen as the intermolecular potential in computer simulations (see Section 1.10). It is not completely realistic, though, because for example it is known that the $1/r^{12}$ form is not a good representation of the repulsive potential. An exponential form $\exp(-r/r_0)$ is better because it reproduces the exponential decay of atomic orbitals at large distances, and hence the overlap which is responsible for repulsions.

Attractive interactions in uncharged molecules result from van der Waals forces, which arise from interactions between dipoles. A molecule has a dipole moment if it contains two opposite charges of magnitude q, separated by some distance $\mathbf{r}$. Such a molecule is said to be polar. The dipole moment is then defined by $\boldsymbol{\mu} = q\mathbf{r}$. Dipole moments of small molecules are usually about 1 debye (D), where $1\text{D} = 3.336 \times 10^{-30}$ C m. Some molecules, such as H_2O, possess a permanent dipole moment due to charge separation resulting from the electro-negativity of the oxygen atom. Dipolar molecules can also induce dipole moments in other molecules producing dipole–induced dipole forces. The potential energy between two dipoles can be calculated by summing up the Coulomb potential energy between each of the four charges. Recall that the Coulomb potential energy is given by

$$V(r) = \frac{q_1 q_2}{4\pi\varepsilon_0 r} \tag{1.3}$$

where r is the distance between charges q_1 and q_2 and ε_0 is the vacuum permittivity.

Considering two parallel dipoles, the potential can be shown to vary as $1/r^3$. However, if the dipoles are freely rotating, the potential varies as $1/r^6$. Further details of the derivations of these functional forms are provided by Atkins (2006). Here we have only discussed the dependence of the potential on r; all prefactors are omitted. This type of relationship is an example of a scaling law, discussed in more detail in Section 1.7.

Most molecules are non-polar. It is evident, however, that there must be attractive van der Waals interactions between such molecules in order that condensed phases, such as those exhibited by liquid hydrogen or argon at low temperature, can exist. Molecules without a permanent dipole moment can possess an instantaneous dipole moment due to fluctuations in the atomic electron distribution. These fluctuating dipoles can induce dipoles which create a transient electric field that can polarize nearby molecules, leading to an induced dipole. Such induced dipole–induced dipole forces create dispersion interactions, also known as London interactions. It is again found that the potential varies as $1/r^6$. In other words, for both freely rotating dipole–dipole and induced dipole–induced dipole interactions, the attractive potential takes the form

$$V(r) = -\frac{C}{r^6} \tag{1.4}$$

although the term C is different for the two types of interaction (further details are provided by Atkins, 1998, for example). This explains why the attractive contribution to the total potential is often taken to have the $1/r^6$ form, as in the Lennard–Jones (12,6) potential (Eq. 1.2) for example.

Coulombic forces dominate other interactions in systems containing ions. This is because the Coulombic potential energy falls off much more slowly (as $1/r$, Eq. 1.1) than any dipole–dipole interaction. A typical Coulombic potential energy is $\sim$250 kJ mol^{-1}, whereas a van der Waals energy is about 1 kJ mol^{-1} or less.

An important distinction can be made between materials in which the structure comes from intermolecular ordering and those for which it is produced by the ordering of molecular aggregates. Many soft materials, such as colloids and micellar amphiphiles, belong to the latter class. A necessary condition for the formation of such aggregates is the existence of at least two components in the system. Often the second component is water and then *hydrogen bonding* interactions are important. In fact, hydrogen bonding is predominantly a type of dipole–dipole interaction, although there may also be some covalent character. For amphiphiles in solution, the *hydrophobic effect* drives the formation of micelles. The hydrophobic effect originates in the local structuring of water, which consists of a tetrahedral arrangement of hydrogen-bonded molecules. When an insoluble species such as a hydrocarbon is added to the water, this structure has to accommodate itself around each molecule, which produces a reduction in entropy. This is known as the hydrophobic effect. This structuring effect is reduced when the molecules assemble into micelles. The hydrophobic effect is discussed further in Section 4.6.5. We note here that since the hydrophobic effect has its origin in the entropy associated with local hydrogen bonding of water molecules, it ultimately depends on dipole–dipole forces.

Even in systems where structure results from molecular self-assembly into aggregates, it is forces between molecules that drive the self-assembly process, although these can be between molecules of different types. In one-component systems such as thermotropic liquid crystals, ordering can only result from forces between molecules of the same type. It is difficult to make a quantitative statement about the precise form of the potential for any soft material, other than observing that it will be some combination of repulsive short-ranged contributions and attractive long-range contributions.

1.3 STRUCTURAL ORGANIZATION

There are both common and distinct features in the ordering of different types of soft material. The most important feature in common is that the ordering is generally intermediate between that of a crystalline solid and that of a liquid. This lack of crystalline order leads to the ‘soft’ mechanical response of the materials. There may, however, be partial translational and/or orientational order of molecules due to the formation of a mesophase by a thermotropic liquid crystal or an amphiphile in water. Polymer melts and solutions are also classified as ‘soft materials’, although there is no long-range translational or orientational order. However, these phases are distinguished from conventional liquids due to their high viscosity and/or viscoelasticity. The lack of long-range translational order can be expressed in another way: soft material structures are characterized by numerous defects, for example lattice dislocations or disclinations in liquid crystals (discontinuities in orientational order, Section 5.4.1). These defects have a profound effect on flow behaviour.

Another feature common to the ordering of soft materials is the periodicity of the structures formed, typically in the range 1–1000 nm, which corresponds to ‘nanoscale’ ordering. Another term often employed is ‘mesoscopic’

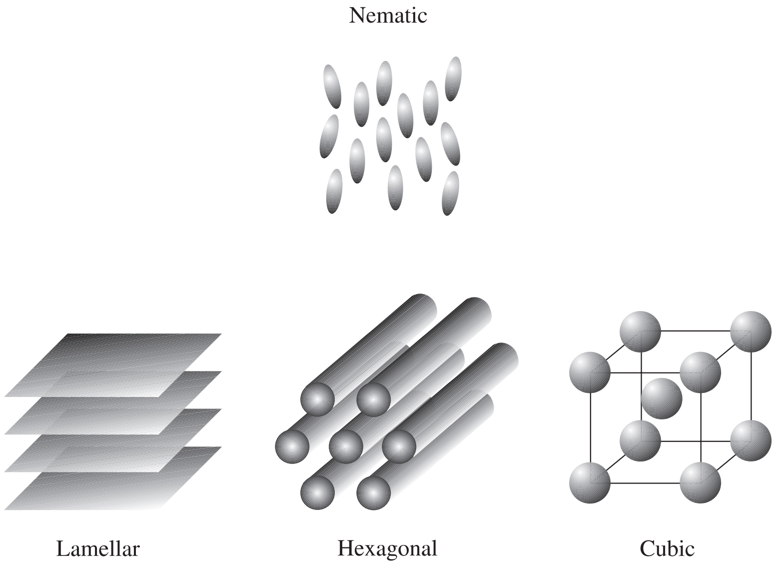

Figure 1.2 Examples of ordering in soft materials. A nematic liquid crystal has no long-range translational order, but the molecules (here shown as ellipses) are orientationally ordered. The lamellar phase has one-dimensional translational order, the hexagonal phase two-dimensional translational order and cubic phases three-dimensional orientational order. The layers in the lamellar phase can be formed from molecules (smectic phase) or amphiphilic bilayers. A hexagonal structure can be formed by disc-like molecules (then being termed columnar phase) or rod-like micelles. The cubic phase shown here is formed by spherical micelles. Bicontinuous cubic structures are also found (see Fig. 4.25d)

ordering. This originates because the length-scale of the structures is intermediate between the microscopic (atomic) and macroscopic scales.

The number of symmetry groups of possible mesophases is restricted. Many types of soft material form structures of the same symmetry, although the molecular ordering may differ. The nematic phase (Section 5.2.2) possesses no long-range translational order, i.e. the molecular order is locally liquid-like. However, there is long-range orientational order (Fig. 1.2). Nematic phases are formed by particles ranging from small organic molecules (~2–3nm long), such as those used in liquid crystal displays, up to long macromolecules, such as rod-like tobacco mosaic virus (~300 nm long).

The simplest structure with translational order is a one-dimensional layered structure (Fig. 1.2). In thermotropic liquid crystals, there are a number of such smectic phases formed by molecules in a weakly layered arrangement (Section 5.2.2). Amphiphiles also form smectic phases, but they are usually called lamellar phases. Here, amphiphile bilayers alternate with layers of solvent (Section 4.10.2). Smectic layered structures are also found in clays, i.e. mineral-based colloidal dispersions.

Phases with two-dimensional translational order are found for both thermotropic and lyotropic liquid crystals, being termed columnar phases for thermotropic liquid crystals and hexagonal phases for lyotropic materials (Fig. 1.2). There is only partial orientational and translational order of molecules within these aggregates. This lower level of molecular order produces a ‘softer’ structure than for hexagonal phases formed by simple molecules or atoms. The hexagonal micellar phase formed by amphiphiles in solution is much softer than graphite, the structure of which is based on a hexagonal arrangement of covalently bonded atoms. The forces between molecules within rod-like micelles and those between amphiphilic molecules and solvent molecules are both much weaker than those involved in covalent bonding and the structure is much less tightly held together. In addition, the van der Waals forces act over a longer range, so that the structural periodicity is much larger. Hexagonal phases are also formed in concentrated solutions of biological macromolecules such as DNA (Section 6.3.1).

Structures with three-dimensional translational order include micellar cubic phases (Fig. 1.2) and bicontinuous cubic phases. These are distinguished topologically (Section 4.9). Micelles are discrete, closed objects within a matrix of solvent. In bicontinuous structures, space is divided into two continuous labyrinths. For lyotropic liquid crystal phases, cocontinuous water channels are divided from each other by a surfactant membrane in one type of bicontinuous structure (in the other, the positions of water and surfactant are reversed). These cubic phases are, on symmetry grounds, crystalline solids. However, unlike atomic or molecular crystals, they are built from supermolecular aggregates, i.e. micelles or surfactant membranes. Thus, as for hexagonal structures, these phases are softer than their atomic/molecular analogues, which are held together by shorter-range forces. Structures with one-, two- and three-dimensional order are also formed by block copolymers, which are polymers formed by linking two or more chemically distinct chains (Section 2.11).

The difference between direct ordering of molecules and the ‘indirect’ ordering of molecules via supermolecular aggregates is one of the distinctions between different types of soft material. Thermotropic liquid crystal phases result from partial orientational and translational order of the molecules. In contrast, the symmetry of lamellar, micellar and bicontinuous phases is specified by the location of supermolecular aggregates. The molecules within the aggregate do not have the same orientational and translational order as the mesoscopic structure itself; in fact, they can be relatively ‘disordered’.

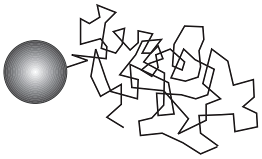

Figure 1.3 Brownian motion of a colloidal particle results from molecular collisions, leading to a path that is a random walk. The statistical analysis for the conformation of a Gaussian polymer chain is the same (Section 2.3.2)

1.4 DYNAMICS

Macromolecules, colloidal particles and micelles undergo Brownian motion. This means that they are subjected to random forces from the thermal motion of the surrounding molecules. This jostling leads to a random zig-zag motion of colloidal particles, which can be described as a random walk (Fig. 1.3). Einstein analysed the statistics of a random walk and showed that the root-mean-square displacement at time t is given by

$$\bar{x} = (2Dt)^{1/2} \tag{1.5}$$

where D is the diffusion coefficient. The motion of colloidal particles in a medium gives rise to a frictional (or drag) force, which is proportional to velocity, at least if the particles are smooth and the velocity is not too great:

$$F = fv \tag{1.6}$$

Here f is the frictional coefficient and v is the velocity. The diffusion coefficient and frictional coefficient are related to kinetic energy via

$$Df = k_B T \tag{1.7}$$

where $k_B T$ is an estimate of the translational kinetic energy per particle, k_B being the Boltzmann constant. Here f for a spherical particle is given by Stokes' law,

$$f = 6\pi\eta R \tag{1.8}$$

where R is called the hydrodynamic radius of the particle (i.e. the effective radius presented by the particle to the liquid flowing locally around it). Equations (1.7) and (1.8) together lead to the Stokes–Einstein equation for the diffusion of a spherical particle,

$$D = \frac{k_{\mathrm{B}}T}{6\pi\eta R} \tag{1.9}$$

Typical diffusion coefficients for molecules in liquids (and thermotropic liquid crystals) are $D \approx 10^{-9}\ \mathrm{m}^2\ \mathrm{s}^{-1}$. Polymers are larger (i.e. they have a larger hydrodynamic radius) and so move much more sluggishly and the diffusion coefficient can be as low as $D \approx 10^{-18}\ \mathrm{m}^2\ \mathrm{s}^{-1}$. Micelles diffusing in water at room temperature with a hydrodynamic radius $\approx$10 nm have $D \approx 2 \times 10^{-11}\ \mathrm{m}^2\ \mathrm{s}^{-1}$.

Translational diffusion of particles in the presence of a non-equilibrium concentration gradient can often be described by Fick's first law. This states that the flux (flow), j, of material across unit area, A, is proportional to the concentration gradient:

$$j = \frac{1}{A}\frac{\mathrm{d}n}{\mathrm{d}t} = -D\frac{\mathrm{d}c}{\mathrm{d}x} \tag{1.10}$$

Here j is the flux, n is the amount (number of moles) of substance and $\mathrm{d}c/\mathrm{d}x$ is the concentration gradient along direction x. Fick's first law applies when the concentration gradient is constant in time. This is often, however, not the case. As diffusion occurs, the concentration gradient itself changes. Fick's second law may then be applicable:

$$\frac{\mathrm{d}c}{\mathrm{d}t} = D\frac{\mathrm{d}^2c}{\mathrm{d}x^2} \tag{1.11}$$

1.5 PHASE TRANSITIONS

Phase transitions can be classified according to whether they are first or second order, this classification originally being introduced by Ehrenfest. Changes in various thermodynamic properties, as well as an order parameter, ψ (Section 1.6), for first- and second-order phase transitions as a function of temperature are illustrated in Fig 1.4. A first-order transition is defined by discontinuities in first derivatives of chemical potential. Enthalpy, entropy and volume can all be defined by appropriate first derivatives of chemical potential and all change discontinuously at a first-order phase transition. The heat capacity is defined as the derivative of enthalpy with respect to temperature. It is thus infinite for a first-order transition. The physical meaning of this is apparent when the boiling of water is considered. Any heat absorbed

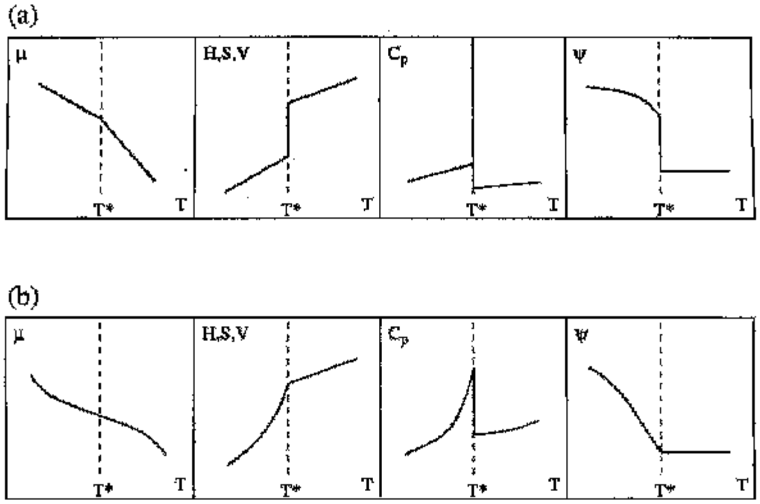

Figure 1.4 Variation of thermodynamic quantities and order parameter with temperature for (a) a first-order phase transition and, (b) a second-order phase transition. The notation is as follows: μ, chemical potential; H, enthalpy; S, entropy; V, volume; C_p, heat capacity (at constant pressure); ψ, order parameter. The phase transition occurs at a temperature $T = T^*$

by the system will drive the transition rather than increasing the temperature, i.e. there is an infinite capacity for absorption of heat. A second-order phase transition is characterized by a continuous first derivative of chemical potential, but a discontinuous second derivative. Thus, enthalpy, entropy and volume all change continuously, although their slopes are different above and below the transition (Fig. 1.4). The heat capacity associated with a second-order phase transition is therefore finite.

Phase transitions are defined thermodynamically. However, to model them, we must turn to theories that describe the ordering in the system. This is often done approximately, using the average order parameter (here we assume one will suffice to describe the transition) within a so-called *mean field theory*. The choice of appropriate order parameter is discussed in the next section. The order parameter for a system is a function of the thermodynamic state of the system (often temperature alone is varied) and is uniform throughout the system and, at equilibrium, is not time dependent. A mean field theory is the simplest approximate model for the dependence of the order parameter on temperature within a phase, as well as for the change in order parameter and thermodynamic properties at a phase transition. Mean field theories date back to when van der Waals introduced his equation of state for the liquid–gas transition.

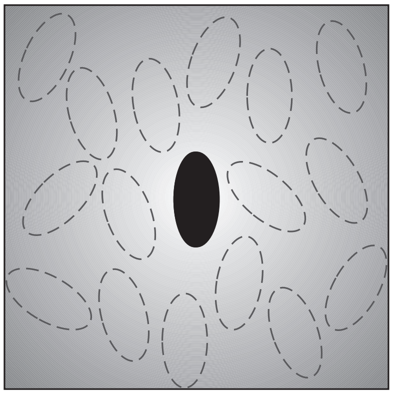

Figure 1.5 In a molecular mean field theory, one molecule (here dark) is assumed to interact with all the others through an average field (symbolized here by grey contours)

In this section we consider a general model that has broad applicability to phase transitions in soft materials: the *Landau theory*, which is based on an expansion of the free energy in a power series of an order parameter. The Landau theory describes the ordering at the mesoscopic, not molecular, level. Molecular mean field theories include the Maier–Saupe model, discussed in detail in Section 5.5.2. This describes the orientation of an arbitrary molecule surrounded by all others (Fig. 1.5), which set up an average anisotropic interaction potential, which is the mean field in this case. In polymer physics, the Flory–Huggins theory is a powerful mean field model for a polymer–solvent or polymer–polymer mixture. It is outlined in Section 2.5.6.

The Landau theory applies to 'weak' phase transitions, i.e. to continuous phase transitions or to weakly first-order transitions, where the enthalpy/entropy change is small. The order parameter is thus assumed to be 'small'. It is a characteristic of soft materials that phase transitions are often weak. It should be mentioned in passing that the Landau theory has been applied to phase transitions in other systems, such as magnets and superconductors. However, here we consider it in the context of a phase transition in a soft material forming a low symmetry phase at low temperature and a high symmetry phase at high temperature. Such a transition is characterized by a change in an appropriate order parameter, denoted ψ, examples of which include an orientational order parameter for nematic liquid crystals (Section 5.5.1) or the composition of a diblock copolymer (Section 2.11). As shown in Fig. 1.4, for a first-order phase transition, the order parameter changes discontinuously, whereas for a second-order phase transition it decreases continuously at the transition. The Landau theory considers changes in free energy density (i.e. Gibbs energy per unit volume) at the phase transition. The essential idea of the theory is that under these conditions, the free energy density can be expanded as a power series in the order parameter:

$$f(\psi, T) = f_0(T) + A(T)\psi + B(T)\psi^2 + C(T)\psi^3 + D(T)\psi^4 + \dots \tag{1.12}$$

Here $f_0(T)$ is the free energy of the high-temperature phase, with respect to which the free energy is defined. The symmetry of the phases under consideration imposes constraints on the number of non-zero terms in this expansion, as illustrated by the following examples. It should be noted that ψ here is associated with a particular state of the system, the equilibrium value $\langle\psi\rangle$ being defined by the minimum of the free energy.

We now consider a second-order phase transition. Simple examples include the smectic C–smectic A transition, which is characterized by a continuous decrease in an order parameter describing molecular tilt. The smectic A (lamellar)–isotropic transition can also be second order under certain conditions. In this case symmetry means that terms with odd powers of ψ are zero. To see this consider the smectic C–smectic A transition. The appropriate order parameter is given by Eq. (5.23) and is a complex quantity. However, the free energy density must be real; thus only even terms $\psi\psi^*$ and $(\psi\psi^*)^2$, etc., remain. Then the free energy can be written as

$$f(\psi, T) = f_0(T) + B(T)\psi^2 + D(T)\psi^4 + \cdots \tag{1.13}$$

Truncation of this expansion at the fourth-order term does not lead to a loss of generality in the essential physics describing a phase transition. Typical curves according to the power series Eq. (1.13) are plotted in Fig. 1.6. Above the transition temperature, T^*, the free energy curve has a single minimum at $\psi = 0$. However, below T^*, minima in free energy occur for non-zero values of ψ, as expected (Fig. 1.6). These curves are obtained with $B(T)$ positive above the transition, but negative below the transition. At the transition $B(T = T^*)$ must vanish, and the simplest function to satisfy these conditions is

$$B(T) = b(T - T^*) \tag{1.14}$$

In addition, the coefficient of the quartic term should be positive, in order to obtain a stable phase below the transition. Although *D(T)* may vary with temperature, it is usually assumed that this dependence is weak, so that *D(T)* can be taken to be a constant, D. We also assume that $f_0(T)$ is not

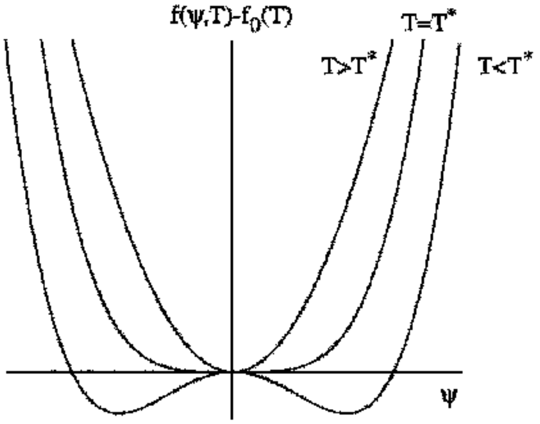

Figure 1.6 Curves of free energy with respect to that of the high-temperature phase, $f(\psi, T) - f_0(T)$, as a function of order parameter ψ, plotted according to the Landau theory for second-order phase transitions. The symmetry-breaking phase transition on reducing temperature is signalled by the development of a non-zero order parameter. At $T > T^*$, the equilibrium value $\langle\psi\rangle = 0$. $T = T^*$ defines the phase transition. At $T < T^*$, the equilibrium value $\langle\psi\rangle \neq 0$

strongly temperature dependent in the vicinity of the transition. Then the temperature dependence of the free energy is determined only by *B(T)*.

To find the equilibrium states, the minima in the free energy are located by differentiating it with respect to the order parameter and setting this equal to zero. The resulting cubic equation

$$2b(T - T^*)\psi + 4D\psi^3 = 0. \tag{1.15}$$

has solutions

$$\psi = 0 \tag{1.16}$$

and

$$\psi = \pm\left(\frac{b}{2D}\right)^{1/2} (T^* - T)^{1/2} \tag{1.17}$$

Above T^*, the only real solution is $\psi = 0$. This corresponds to the state with an equilibrium value $\langle\psi\rangle = 0$. However, for temperatures below T^*, $\psi = 0$ corresponds to a maximum in the free energy (see Fig. 1.6) while the solutions $\psi = \pm(b/2D)^{1/2}(T^* - T)^{1/2}$ are the symmetrically placed minima. The magnitude of the equilibrium order parameter in the low-temperature phase therefore decreases with increasing temperature according to

$$\langle \psi \rangle = \left(\frac{b}{2D} \right)^{1/2} (T^* - T)^{1/2} \tag{1.18}$$

The exponent $\frac{1}{2}$ for the temperature dependence is characteristic of mean field behaviour.

The second-order nature of the transition is confirmed since the entropy change at the transition is zero. This can be shown by calculating the entropy density (at constant volume), s:

$$s = -\left(\frac{\partial f}{\partial T} \right)_v \tag{1.19}$$

Above the phase transition this takes the value

$$s = s_0 \tag{1.20}$$

whereas below the transition,

$$s = s_0 + \left(\frac{b^2}{2D} \right) (T - T^*) \tag{1.21}$$

This shows that the entropy density decreases continuously to zero as the phase transition is approached, i.e. there is no discontinuity in entropy.

A similar analysis can be made for the Landau free energy of a weakly first-order phase transition, for example the nematic-isotropic transition exhibited by some liquid crystals (Section 5.7.1). The free energy (Eq. 1.13), is supplemented by an additional cubic term $C(T)\psi^3$ if the transition is first order. The first-order nature of the transition can be confirmed by calculating the entropy density change at the transition, which turns out to be

$$\Delta s = -\frac{bC^2}{4D^2} \tag{1.22}$$

i.e. it is finite. Confirmation of this result is left as an exercise for the interested reader.

Mean field theory provides a basis for understanding many soft materials. The Landau theory is one example of a mean field theory that we have highlighted because of its generality in describing, at least qualitatively, phase transitions in weakly ordered systems. Other types of mean field theory have been used to model specific soft materials, but we do not have the space here to list them all.

Going beyond mean field models, the next level of theoretical approximation is to allow for (usually thermal) fluctuations around the mean system configuration. These fluctuations are considered to be a weak 'perturbation' with respect to the average order. Unfortunately, many soft materials are strongly fluctuating, especially near to a phase transition, and this approach then breaks down. This is not too much of a concern, however, because just as for atomic systems, more sophisticated perturbation theories are sure to be developed for soft materials.

1.6 ORDER PARAMETERS

Phase transitions in condensed phases are characterized by symmetry changes, i.e. by transformations in orientational and translational ordering in the system. Many soft materials form a disordered (isotropic) phase at high temperatures but adopt ordered structures, with different degrees of translational and orientational order, at low temperatures. The transition from the isotropic phase to ordered phase is said to be a symmetry breaking transition, because the symmetry of the isotropic phase (with full rotational and translational symmetry) is broken at low temperatures. Examples of symmetry breaking transitions include the isotropic–nematic phase transition in liquid crystals (Section 5.5.2) and the isotropic–lamellar phase transition observed for amphiphiles (Section 4.10.2) or block copolymers (Section 2.11).

Symmetry breaking phase transitions are characterized by a change in one or more order parameters that describe the average order in the system. In general, we can define an order parameter at a point r in the system as

$$\langle \psi(\mathbf{r}) \rangle = \int \psi(\mathbf{r}) f\,[\psi(\mathbf{r})]\mathrm{d}\mathbf{r} \tag{1.23}$$

where $f(\psi)$ is the appropriate distribution function for an orientational or translational variable.

For the isotropic–nematic phase transition, the appropriate order parameter quantifies the average degree of orientational order in the low-temperature phase. It is denoted $\bar{P}_2$, as defined by Eq. (5.11) (this order parameter only quantifies the 'first moment' of the orientational distribution function; higher-order parameters can also be defined, as discussed in Section 5.5.1).

A phase transition from an isotropic phase to a lamellar (smectic) phase is defined by the development of translational order in one dimension. The layered structure is characterized by a periodic alternation in density or composition. An order parameter that accounts for both the phase and amplitude of the layer order is defined by Eq. (5.23). This order parameter is a vector, because the layer normals lie along a particular direction in three-dimensional space. Order parameters for phase transitions where there is a change in translational order only are vectors, whereas those associated with changes in orientational order alone are generally tensors. The orientational ordering tensor is a matrix that relates the orientation of a molecule-fixed axis system to a laboratory-fixed coordinate system (Eq. 5.13). The order parameter $\bar{P}_2$ that is itself a scalar is equivalent to one element of the orientational ordering tensor, as discussed in Section 5.5.1.

1.7 SCALING LAWS

Soft matter is characterized by complexity, both in structure and dynamics. Theories for these materials are thus difficult, and in many cases not quantitative. However, it is still instructive to consider how one variable depends on another, holding other quantities constant. This leads to so-called *scaling laws*, where numerical constants are omitted, but the interrelationship of quantities is established. Sometimes scaling laws can simply be deduced from dimensional arguments, i.e. by balancing the dimensions of quantities on both sides of an equation. Scaling relationships are important in the physics of soft matter, and many universal relationships can be established using them. Examples of scaling laws are given for polymer solutions in Section 2.5.1. Another example is provided by much of the discussion of intermolecular interactions in Section 1.2, where the dependence of intermolecular potential on intermolecular separation was expressed as a power law, but without specifying an equation with precise numerical constants. A simple scaling law might look something like

$$x \sim y^z \tag{1.24}$$

which should be read as x ‘scales with’ y to the power z. In estimating numerical quantities, the symbol $\sim$ reads ‘of the order of’ and in this book is interpreted to mean roughly within an order of magnitude.

1.8 POLYDISPERSITY

Unlike atoms and molecules in hard solids, colloidal particles, polymer chains and micelles are all characterized by a distribution of sizes known as *polydispersity*. Polydispersity has important consequences for the structure and dynamics of soft materials. It can influence phase behaviour; for example polydispersity of polymer chain length (Section 2.4.1) leads to phase separation in solutions or blends into phases rich in the small and large polymer species. Indeed, this is the basis of fractionation methods used to determine the distribution of polymer molar masses. Here a non-solvent is added to a dilute polymer solution until phase separation occurs. The critical temperature for phase separation will be reached first for large polymer chains, which can then be separated from the shorter chains remaining in solution. Another case that illustrates the effect of polydispersity on thermodynamics is provided by the crystallization of colloidal latex particles at large volume fractions (Section 3.15). This can be suppressed if the particles are polydisperse, an effect that has been modelled using binary mixtures of particles with different sizes.

A good example of the effect of polydispersity on a kinetic process is provided by polymer adsorption on to a solid substrate. If a solution of an adsorbing polymer is exposed to a substrate, then thermodynamically it is favourable for the larger chains to be adsorbed first. However, the diffusion coefficient is greater for small chains, so that in fact these are the first to adsorb. Thus, initially there is a non-equilibrium state of preferential adsorption of small chains. The subsequent exchange of small chains by large ones can be very slow (as long as hours or days) and this process, resulting from polydispersity, is the rate-determining step. It is important when coating a surface with paint, for example.

1.9 EXPERIMENTAL TECHNIQUES FOR INVESTIGATING SOFT MATTER

1.9.1 Microscopy

The mesoscopic length-scale of soft materials means that optical microscopy is usually not a suitable method for examining their detailed structure, although it can be used to view colloidal particles around 1 μm in size. However, polarized optical microscopy is useful for identifying birefringent structures formed by liquid crystals (thermotropic and lyotropic) such as the various types of smectic (lamellar) or discotic (hexagonal) structures. Here, textures that result from defects in the structure are imaged, rather than the actual microstructure itself. Optical microscopy can also be used to examine the macroaggregates formed by polymers, such as spherulites. Some colloidal particles are large enough to be observed directly in the optical microscope via *differential interference contrast (DIC) microscopy*. This relies on the interference between light waves reflected through different (thickness/birefringence) regions of the specimen.

Electron microscopy provides structural information to subnanometre resolution, and is thus used to image soft matter, with a restriction to 'dry' materials imposed by the requirement to maintain a high vacuum in the microscope. There are two main classes of electron microscopy. *Scanning electron microscopy* (SEM) images the exterior of an object. Here an electron beam is scanned across an object, knocking secondary electrons out of its surface atoms. These are then detected and form the image. In *transmission electron microscopy* (TEM), the intensity of transmitted electrons is inversely proportional to the electron density of a section of material through which it has passed. The method requires sectioning of a bulk sample into nanometre-thick slices. TEM offers a higher resolution than SEM, typically being able to resolve 1 nm features compared to 5 nm for the latter. Unfortunately, the electron density contrast within many soft materials is insufficient on its own, and the samples thus have to be stained. This is achieved using vapours of heavy atom oxides such as osmium tetraoxide which react selectively with unsaturated bonds. TEM is used to examine sections of biological materials (for example cell membranes) as well as microstructures formed by block copolymers.

1.9.2 Scattering Methods

Light scattering

In static light scattering, the intensity of elastically scattered light is measured as a function of scattering angle, θ. When scattering at small angles is probed, the technique is called *small-angle light scattering* (SALS). Light scattering can be analysed on the basis of diffraction from point scatterers when the particles are much smaller than the wavelength, $d \ll \lambda$ (usually taken to be $d < \lambda/20$). This defines so-called *Rayleigh scattering*. If the particle is smaller than the light wavelength, but not too much, i.e. $d < \lambda$, we are in the Rayleigh–Debye–Gans regime and the analysis of scattering is more complex. Here the scattered intensity is different in the forward and back scattering directions (for example it is different at 45° than at 135°), and the ratio I_{45}/I_{135} can be used to determine the particle size. The angular variation of light intensity can also provide information on particle shape, whether Gaussian polymer coils, rigid rods or micelles. In *Mie scattering*, the particle size is comparable to the wavelength of the light. The Mie analysis accounts for systems where there is also a large difference in refractive index between particles and dispersion medium. It should be noted that there is an overlap in the range of wavenumbers accessible in SALS and either small-angle x-ray or neutron scattering experiments (to be discussed shortly) from soft materials, and one or other may be suitable depending on the size of the particles.

Many polymer molecules are big enough for interference to occur between waves scattered by different parts of the molecule. This means that light scattering can be used to measure the overall dimensions of polymer chains or associates such as micelles.

Dynamic light scattering (DLS) is used to study diffusion in polymer solutions. It is sometimes known as photon correlation spectroscopy (PCS) or quasi-elastic light scattering (QELS). It involves measuring the temporal fluctuations of the intensity of scattered light. The number of photons entering a detector are recorded and analysed by a digital correlator. The separation in time between photon countings is the correlation time. The autocorrelation function of the intensity at an angle θ can be analysed to yield the distribution of relaxation times. The decay rates of the relaxation modes provide translational diffusion coefficients. From these, the hydrodynamic radius of the constituent particles can be obtained using the Stokes–Einstein equation (Eq. 1.9). Because the intensity of scattered light is z-weighted ($z \propto cM_w$ where $c =$ mass concentration and $M_w =$ mass-average molar mass), DLS is sensitive to low levels of high molar mass solutes.

X-ray and Neutron scattering

Because x-ray and neutron beams have much smaller wavelengths than light, typically 0.1 nm, they can be used in scattering experiments to probe much smaller features than with visible light. Of the two methods, x-ray diffraction can be carried out using instruments in the laboratory whereas neutron diffraction needs a source producing a neutron beam, such as a nuclear reactor or an instrument called a spallation source in which neutrons are produced by bombardment of a metal target by a beam of protons.

X-rays are scattered by electrons so that x-ray diffraction comes from the electron density distribution in a material. X-ray scattering methods may be divided into two groups, depending on the angle θ, where 2θ is the scattering angle (Fig. 1.7). In small-angle x-ray scattering (SAXS) θ is less than about 5°, but in wide-angle x-ray scattering (WAXS) θ is larger than this. The scattering vector $\mathbf{q}$ is also defined in Fig. 1.7. It is the difference between

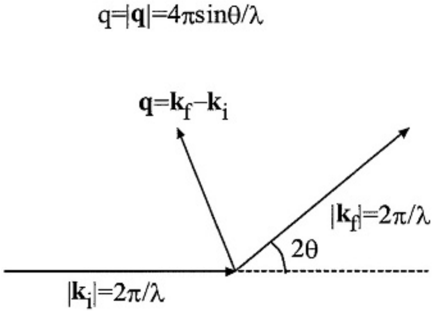

Figure 1.7 Definition of the scattering vector **q** and its magnitude |**q**|. The angle between incident and scattered beams is 2θ and γ is the wavelength of the radiation. The wavevector of the incident beam is denoted $\mathbf{k}_\mathrm{i}$ and that of the scattered beam $\mathbf{k}_\mathrm{s}$

incident and diffracted wavevectors, $\mathbf{q} = \mathbf{k}_\mathrm{s} - \mathbf{k}_\mathrm{i}$. Since $|\mathbf{k}_\mathrm{i}| = |\mathbf{k}_\mathrm{s}|$ for elastic scattering, the magnitude of the wavevector is

$$q = |\mathbf{q}| = \frac{4\pi \sin\theta}{\lambda} \tag{1.25}$$

where λ is the wavelength of the x-rays. The wavevector is a useful quantity because a diffraction peak occurs at a fixed q independent of wavelength, whereas its scattering angle will change with λ.

WAXS provides information on the structure of crystalline polymers via Bragg's law:

$$n\lambda = 2d \sin\theta \tag{1.26}$$

where n is the order of diffraction and d is the spacing between lattice planes. Reflections at different angles θ correspond to diffraction from allowed planes in the lattice, and hence provide information on the unit cell dimensions.

Because Bragg's law shows that θ and d are reciprocally related, it is apparent that small-angle x-ray scattering probes larger structural features than WAXS. It is used to examine structures with sizes ranging from 5 nm up to 100 nm. Thus, it can be used to measure the radius of gyration (Section 2.3.2) of polymers in solution. For such systems the scattering at small angles obeys Guinier's law, where the intensity varies as

$$I(q) = I(0)\exp\left(-q^2 R_\mathrm{g}^2/3\right) \tag{1.27}$$

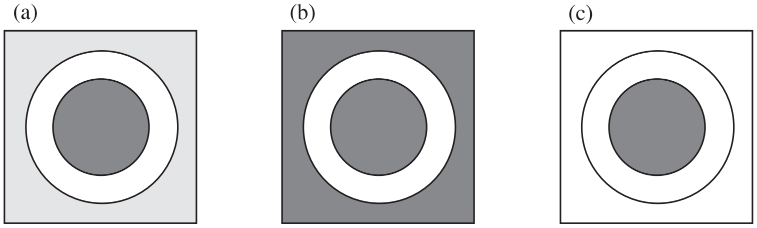

Figure 1.8 Schematic illustrating the contrast matching technique used in small-angle neutron scattering experiments. Micelles are formed by amphiphiles with a deuterated solvophobic chain and normal protonated solvophilic headgroup. Each micelle then has a deuterated core (dark) and protonated corona (white), (a) The solvent is a mixture of normal and deuterium-labelled molecules, and there is contrast between the solvent and both the core and corona of the micelle. (b) By increasing the proportion of deuterated molecules in the solvent, the core is 'contrast matched', and only the corona scatters neutrons. (c) By reducing the proportion of deuterated molecules in the solvent, the corona can be contrast matched to the solvent. Then only scattering from the core is obtained

Here $I(0)$ is the intensity at $q = 0$. A plot of $\ln[I(q)]$ versus q^2 yields the radius of gyration, R_g.

Small-angle neutron scattering (SANS) is based on the same principles as SAXS. However, neutrons are scattered by atomic nuclei and neutron diffraction depends on the nuclear scattering length density. The scattering length indicates how strongly the nucleus scatters neutrons (it is a measure of its effective size in a collision with a neutron). Importantly, it does not depend systematically on atomic number (whereas the electron density relevant to x-ray scattering does). In fact, the scattering length for a hydrogen nucleus ^{1}H is completely different to that for a deuterium nucleus ^{2}H. This leads to the major use of SANS in studying polymers and soft matter. We can change the scattering power of labelled parts of a material by substituting ^{1}H for ^{2}H. A good example to show the principle of the method is shown in Fig. 1.8. Here the method is illustrated using the example of a micelle, where it is possible to isolate scattering from either the micellar corona or core only by changing the contrast of the solvent, i.e. by varying the proportions of normal and deuterated molecules. Here we imagine that the solvent initially consists of both types of molecule; the hydrophobic parts of the amphiphilic molecule are deuterium labelled, whereas the hydrophilic parts are not. In this case, the solvent, corona and core each have a different scattering density (Fig. 1.8a). However, if we increase the proportion of deuterated molecules in the solvent, it is possible to reach a condition termed *contrast matching*, where the solvent and core have the same scattering amplitude. Then by Babinet's principle, we only detect the scattering of the corona

(Fig. 1.8b). Similarly, by changing the contrast of the solvent to match that of the corona, scattering occurs only from the core (Fig. 1.8c). In practice, contrast is achieved through some combination of labelling of the solvent, corona and core. The matching conditions can be calculated using the known scattering densities for the species. SANS with contrast matching has also been used to investigate the dimensions of selectively labelled parts of polymer chains and to measure the total radius of gyration of polymer chains in the melt.

The distribution of intensity of scattered radiation in a diffraction pattern is related by a Fourier transformation to the autocorrelation function of scattering density, $\langle \rho(r)\rho(r')\rangle$, where $\langle \cdots \rangle$ indicates an average over the sample. In crystallography the autocorrelation function is known as the Patterson function. It is very useful to factor out contributions to the total intensity from interfering waves scattered by single particles and from interparticle interferences:

$$I(q) = k(\Delta\rho)^2 P(q)S(q) \tag{1.28}$$

Here k is a constant that accounts for geometrical effects and scattering volume and $(\Delta\rho)^2$ is the scattering contrast between the polymer and solvent (i.e. the difference in electron densities in the case of x-ray scattering). Here $P(q)$ is the single particle scattering term (the square of the *form factor*) and $S(q)$ is the interparticle scattering term, known as the *structure factor*. Equation (1.28) is strictly only valid for a collection of spherical particles, but provides a good approximation in other situations as long as the particles are not too anisotropic.

The form factor and structure factor can often be separated. Then we can obtain information on the particle size and shape from $P(q)$ using appropriate models. Modelling is necessary because the density distribution within a particle cannot be obtained directly due to the phase problem, i.e. information on the phase shift of waves upon diffraction is lost because intensities are measured. The structure factor is related by a Fourier transformation to the radial distribution function, $g(r)$:

$$S(q) = 1 + \frac{N}{V}\int [g(r) - 1]\exp(i\mathbf{q}\cdot\mathbf{r})\mathrm{d}\mathbf{r} \tag{1.29}$$

where N/V is the number of particles per unit volume. The radial distribution function reflects the interparticle ordering; specifically $g(r)r^2\mathrm{d}r$ is the probability that a molecule is located in the range dr at a distance r from another. The radial distribution function gives a picture of the extent of translational order in the system (see Fig. 5.9, for example). It can be obtained

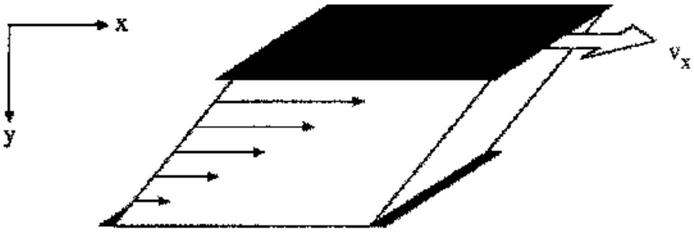

Figure 1.9 A simple shear deformation. The top plate is moved at constant speed v_x, causing a steadily increasing strain

from diffraction experiments, using Eq. (1.29) if the structure factor can be isolated.

1.9.3 Rheology

Rheology is the science of the deformation and flow of matter. It provides information on the mechanical response to a dynamic stress or strain. Recall that stress (σ) is the force per unit area and so has units N m^{-2} or Pa. Strain (ε) is the relative change in length of the sample and is dimensionless. A simple shear deformation is illustrated in Fig. 1.9. The bottom plate is fixed but the top plate is moved at a speed v_x in the x direction. If the gap between the plates is filled with a simple liquid like water, it is observed that the shear stress is proportional to the velocity gradient $\mathrm{d}v_x/\mathrm{d}y$:

$$\sigma = \eta \frac{\mathrm{d}v_x}{\mathrm{d}y} \tag{1.30}$$

The constant of proportionality is the viscosity, η. It has units of kg m^{-1} s^{-1} or Pa s. Another unit sometimes used is poise, where 1 poise = 0.1 Pa s. As a reference, water has a viscosity of 10^{-3} Pa s.

In practice, viscosity is measured by applying a steady or oscillating stress or strain. Then we can define $\dot{\gamma} = \mathrm{d}v_x/\mathrm{d}y$ as the shear rate in units of s^{-1}. When the shear stress is proportional to the shear rate,

$$\sigma = \eta\dot{\gamma} \tag{1.31}$$

and the viscosity is independent of shear rate, the fluid is said to be *Newtonian*.

However, many fluids do not have a viscosity that is a constant, independent of shear rate. Such systems exhibit non-Newtonian flows. Many

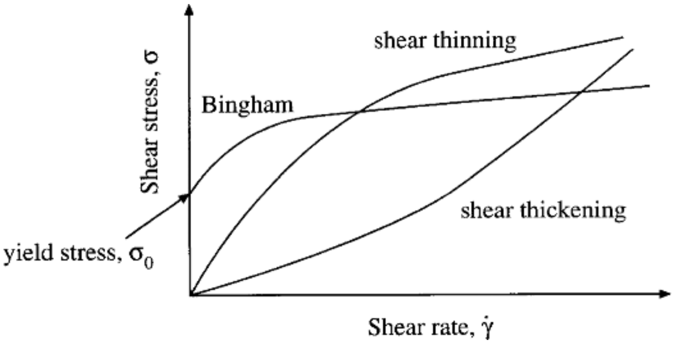

Figure 1.10 Illustrating non-Newtonian flow behaviours. For a Newtonian fluid, the shear stress is proportional to the shear rate. In contrast, there are non-linear dependencies of shear stress on shear rate if shear thickening or shear thinning occur. A Bingham fluid has a finite yield stress

everyday materials like paint or yogurt get thinner as the shear rate is increased—this is termed *shear thinning*. Some things become thicker with increasing shear rate and are *shear thickening*, for example whipped cream. Other substances are plastic above a certain shear stress, which means that they undergo irreversible flows. Fluids that do not exhibit plastic flow until a yield stress, σ_0, are called Bingham fluids and the stress is given by

$$\sigma = \eta\dot{\gamma} + \sigma_0 \tag{1.32}$$

Non-Newtonian flow behaviours are illustrated in Fig. 1.10.

In contrast to liquids, solids have an elastic response to applied stress or strain, at least for small deformations. An elastic object is one that returns to its original shape if the force is removed. At low strains, the stress is proportional to strain (Hooke's law) and independent of the deformation rate.

Just as the structural properties of soft materials have some elements of a liquid and some elements of a solid, the flow or rheological properties do too. A good example of this is 'silly putty', which is a rubbery polymer called silicone. This will flow out of a container like a liquid. However, if it is formed into a ball and dropped on the floor, it bounces back, i.e. it behaves like an elastic material. The crucial factor is the time for which the force is applied. Pouring is a slow flow due to gravitational forces, but the brief impact of the ball with the floor means the force acts for an instant. One of the most important characteristics of soft materials is the dependence of mechanical behaviour on the rate of deformation. Because at low rates of deformation most soft materials exhibit viscous behaviour whereas at high rates of deformation they behave elastically, they are called *viscoelastic* materials. The characteristic time-scale of a material is called its *Deborah number*, defined as the ratio of a relaxation time τ to a time constant t_f defining the flow: De $= \tau/t_{\mathrm{f}}$. For example, for oscillatory shear, t_{f} is the inverse of the oscillation frequency, ω, so that De $= \tau\omega$. When the flow is fast compared to the relaxation time of the soft material, De $\gg 1$, it behaves as a solid, whereas for De $\ll 1$, the response is liquid-like. Other dimensionless parameters are defined in a similar way to the Deborah number. For steady shear, the Weissenberg number is often used. It is defined as Wi $= \dot{\gamma}\tau$ where $\dot{\gamma}$ is the shear rate. Non-linear flow effects are prominent when Wi > 1. For colloidal suspensions, the Peclet number is used, defined as Pe $= \dot{\gamma}\tau_{\mathrm{D}}$, where τ_{D} is a characteristic diffusion time.

The viscoelasticity of soft materials is probed via several types of experiment. In stress relaxation measurements, the strain is held constant and the decay of stress is monitored as a function of time. Usually the rate of decay decreases as time progresses. In creep experiments, the stress is held constant and the increase in strain is monitored. Generally, the strain increases rapidly at first and then the rate of increase becomes smaller. In addition to these measurements, many commercial rheometers are able to perform dynamic mechanical testing, where an oscillatory strain is applied to the specimen. If the frequency of deformation is ω and t denotes time, we can write the strain as

$$\gamma = \gamma_0 \sin \omega t \tag{1.33}$$

where γ_0 is the amplitude of the strain. For a viscoelastic system, a component of the stress will be in phase with the strain (elastic part), and a component will be out of phase with it (viscous part). We can therefore write

$$\sigma = \sigma_0' \sin \omega t + \sigma_0'' \cos \omega t \tag{1.34}$$

Defining an in-phase shear modulus as

$$G' = \frac{\sigma_0'}{\gamma_0} \tag{1.35}$$

and an out-of-phase shear modulus as

$$G'' = \frac{\sigma_0''}{\gamma_0} \tag{1.36}$$

we obtain

$$\sigma = G'\gamma_0 \sin \omega t + G''\gamma_0 \cos \omega t \tag{1.37}$$

The ratio

$$\tan \delta = \frac{G''}{G'} \tag{1.38}$$

is called the loss tangent, and is a measure of the energy loss per cycle. Often G' is called the storage modulus and G'' the loss modulus, to reflect the energy transfer during the deformation. Being moduli, they both have units of Pa.

There are many designs of rheometer for materials with different viscoelasticities. For example, liquids can be examined in the Couette geometry, which consists of vertical concentric cylinders, one of which rotates with the sample between the gap. Cone-and-plate and parallel disc cells are also widely used. For soft solids, oscillatory shearing between vertical parallel plates yields the dynamic shear moduli.

When a solid sample is subjected to extensional or compressional strain and the stress is measured, it is possible to determine Young's modulus in the region where stress is proportional to strain:

$$E = \frac{\sigma}{\varepsilon} \tag{1.39}$$

An extensional deformation is also known as a tensile deformation. If an oscillatory deformation is applied to a viscoelastic material, a complex modulus with components E' and E'' can be defined, in analogy to the dynamic shear moduli G' and G'' (cf. Eq. 1.37).

If a material is subjected to a constant elongational stress in a creep experiment, the compliance is defined in terms of the time-dependent strain by

$$J(t) = \frac{\varepsilon(t)}{\sigma} \tag{1.40}$$

Measurements of $J(t)$ provide an alternative to the relaxational shear modulus $G(t)$. The latter can be obtained from the dynamic shear moduli by a transformation from frequency to time domains.

1.9.4 Spectroscopic Methods

Nuclear magnetic resonance (NMR)

NMR is a method of probing the motions of nuclei in molecules when they come into resonance with an oscillating magnetic field. It is a local probe of the ordering of magnetic nuclei. Of course, it can be used to identify compounds via analysis of chemical shifts, i.e. the shift in resonance frequency of a nucleus with respect to a reference material. In polymer solutions, ^{1}H and ^{13}C NMR are widely used to determine the number average molar mass and the composition of copolymers by end group analysis (Section 2.4.2). NMR can also be used to probe the local microstructure of polymer chains, for example tacticity, by measuring spectral splittings arising from spin–spin coupling. Lines in NMR spectra become broader as molecular motions get slower, as they do in a solid sample. This broadening provides information on the dynamics of segmental motion. However, decoupling methods have been developed to reduce the effect of this broadening if the interest is in the static local structure of polymers in the solid state.

Using deuterium labelling methods, it is possible to obtain orientational order parameters for C–D bonds via nuclear quadrupolar splittings. This provides information on the orientational ordering of thermotropic liquid crystals and of labelled hydrocarbon chains in amphiphilic aggregates such as micelles and lamellae. As another example, the orientation (and motions) of molecules adsorbed on colloidal particles has been studied.

In addition to being a powerful probe of the static order within a material, NMR has also proved extremely valuable in studying dynamics. Here the relaxation of magnetically excited nuclear spins is followed. There are two types of relaxation process. In spin–lattice relaxation, the energy imparted to the nuclear spins by the magnetic field is transferred to the surroundings (the lattice) to restore the Boltzmann distribution of spin energies. Since the motions of the ‘lattice’ molecules are quite different in liquids and solids, the spin–lattice relaxation time T_1 varies considerably. In spin–spin relaxation, spins relax upon removal of the magnetic field by randomizing their orientation in the plane normal to the magnetic field. The corresponding spin–spin relaxation time is denoted T_2. As mentioned above, the broadening of NMR lines is due to molecular motions; i.e. in principle measurements of line width can be used to obtain T_1 and T_2. However, accurate measurements of T_1 and T_2 are best performed through pulsed NMR spin echo methods. Further details of this can be found elsewhere. For amphiphiles and colloids as well as polymers in dilute solution, NMR can be used to determine the translational self-diffusion coefficient of molecules via such spin relaxation experiments in a pulsed magnetic field gradient. NMR spin relaxation measurements have also provided much information on the local dynamics of segments of a polymer chain or of liquid crystal molecules, for example. In surfactants, similar experiments have shown that the hydrocarbon chains within a micelle undergo motions characteristic of a liquid environment.

Infrared and Raman spectroscopy

Infrared spectroscopy is used to probe vibrational motions of molecules. Infrared radiation is absorbed at discrete frequencies corresponding to energy levels for molecular bond vibrations, when there is an oscillating dipole moment. Absorption of infrared radiation results from a coupling of molecular vibration with the oscillating electric field of the radiation. To be infrared (IR) active, a bond vibration must produce a change in the electric dipole moment of the molecule. Different bond stretching or bending modes (eg. C—H stretch, O—H bend) give rise to absorptions in distinct bands, and this can be used to identify a material. Often this is done using a 'fingerprint' region of a spectrum (usually in the range of wavenumbers 4000–650 cm^{-1}) and comparing this to a known reference specimen. For polymers, IR spectroscopy provides information on chain branching and other aspects of microstructure (tacticity, length of unsaturated groups), as discussed in Section 2.4.2. The presence of hydrogen bonding in polymer, surfactant or colloid solutions can be inferred from changes in the vibrational frequencies of O—H bonds. Infrared *dichroism* measurements are used to probe the absorption of polarized infrared radiation in different directions and can be used to determine information on the orientation of a particular bond (producing a specific vibrational frequency).

Raman spectroscopy is concerned with analysing the frequency shifts of monochromatic microwave or infrared radiation that result from the change in photon energy caused by scattering of radiation due to molecular vibrational or rotational motion respectively. Most of the incident radiation is transmitted through the sample; therefore Raman scattering is a weak effect, which can limit its sensitivity in some applications. In soft materials, Raman scattering is applied to probe specific vibrational bands, which occur in the infrared region of the spectrum. For Raman scattering to be observed, a molecular rotation or vibration must result in some change in molecular polarizability, this mode then being Raman active. Raman spectroscopy can be used like IR spectroscopy to identify particular bonds in a molecule with Raman-active vibrations. Polarized Raman scattering is a method for studying molecular orientational order in soft materials, providing information on the ordering of specific bonds. The intensity of the Raman scattered radiation depends on the orientation of the chemical bond with respect to the polarization direction of the radiation. Raman microscopy is used to obtain information on the orientation of molecules at a surface, by scanning a Raman microprobe across it. Photon correlation spectroscopy is usually understood to refer to visible radiation, but the same method can be used to analyse the fluctuations of Raman (and IR) radiation. This provides information on the dynamics of molecular motions, since molecular rotation will modify the vibrational frequencies. This can be used to determine rotational diffusion coefficients.

Dielectric spectroscopy

This is a useful probe of the motions of polar molecules. When an electric field is applied, the molecules will tend to align along the field direction. Upon release of the electric field, the molecules will relax with a characteristic time which depends on their dynamical interactions with their neighbours. In dielectric spectroscopy, an oscillating voltage is applied to the sample and the variation of the current across it is measured. The magnitude and phase of the current with respect to the input voltage are used to define the complex dielectric constant, ε^*. In many ways, this is analogous to the complex shear (or extensional) modulus measured in rheology experiments (defined in Eqs. 1.34 to 1.37). In particular, ε^* has an in-phase (storage) component, called the dielectric constant (ε', analogous to G'), and an out-of-phase component, termed the dielectric loss (ε'', analogous to G''). The phase shift between them defines a loss tangent, just as in Eq. (1.38). However, dielectric spectroscopy can cover a wider range of oscillation frequencies than dynamic mechanical spectroscopy, up to 15 orders of magnitude from 10^{-5} Hz up to 10^{10} Hz (although all of this range cannot be covered with a single instrument). The ability to cover higher frequencies than rheology is important because it enables the study of molecular motions in polymers. The characteristic frequencies of dipole relaxations in polymers range from 20 Hz to 100 kHz. The higher end is not accessible in rheology experiments, but is important in studying the glass transition and other processes associated with changes in segmental motions (discussed further in Section 2.6.4). Often rheology and dielectric spectroscopy provide complementary information, rheology probing low-frequency dynamics and dielectric spectroscopy high-frequency processes. In liquid crystals, molecular rotational motions are anisotropic, and this has also been studied using dielectric spectroscopy.

UV and visible spectrosopy

These techniques rely on measurements of spectral frequencies resulting from electronic transitions. They can be used to identify molecules, but do not provide information on ordering of soft materials and so are not considered further here.

1.9.5 Calorimetry

Calorimetry is the measurement of heat changes as the temperature of a substance is varied. In a calorimeter in which the sample is held at constant volume, changes in internal energy are detected. If the pressure is constant, then enthalpy changes are measured. In the latter (more usual) experiment, phase transitions are characterized by finite enthalpy changes if they are first order or changes in the gradient of enthalpy with temperature if they are second order (Fig. 1.4).

A common method to locate phase transitions and to determine the associated transition enthalpy in soft materials is *differential scanning calorimetry* (DSC). The differential power necessary to maintain a given temperature for two pans containing the material and a reference sample is recorded. A discontinuous phase transition is indicated by a sharp endotherm or exotherm which causes changes in the differential power supplied to the sample.

1.9.6 Surface Structure Probes

Atomic force microscopy (AFM) is the most commonly used scanning probe microscopy (SPM) technique. It has been demonstrated to be an invaluable technique for characterization of nanoscale surface structures. In this method, the deflection of a cantilever due to repulsive electronic interactions of an attached sharp tip with the surface is measured. The microscopic movement of the tip creates a force that is measured to provide an image of the surface. Both contact and 'tapping' mode AFMs have been employed for the investigation of surface topography, the latter avoiding contact of the tip with the surface, which can be a problem if the material is soft.

The very small (typically piconewton) forces necessary to compress soft materials confined between substrates such as mica have been measured directly using the *surface forces apparatus*. Here, the force is measured as a function of the separation between the plates, which are often in the form of crossed half-cylinders so that the compressed area is minimized. The separation between the plates (from 0 to 10^3 nm) is measured using interference fringes from the mica sheets (silvered on the back) viewed in a light microscope. Surface forces experiments are technically demanding, because to provide information on interparticle forces it is necessary to control the separation of the plates to 0.1 nm or better. In addition, it is very important to keep dust out of the apparatus. Nevertheless, the technique is now successful to the extent that commercial surface forces apparatus is available. An example of the use of surface forces experiments is in the measurement of forces between lipid bilayers. The forces between bare mica sheets provide information on this colloidal material, a type of clay (Section 3.11). This method has also been used to study polymer layers adsorbed on to mica, the resulting force–distance curves mimicking those of sterically stabilized colloid particles as they approach one another.

X-ray or neutron reflectivity experiments involve measuring the intensity of x-rays or neutrons reflected from a surface as a function of angle of incidence (or wavevector magnitude q, Eq. 1.25). The case where the angle of the reflected beam is equal to the incident angle and the plane of reflection is normal to the surface is termed *specular reflectivity*. It provides the scattering density profile normal to the film surface. Below a critical angle for reflection (which is proportional to the average scattering density in the material), all x-rays or neutrons are reflected. Above this critical angle, the reflectivity for a film of uniform density falls off as q^{-4} (Fresnel law). Modulations superimposed on this result from the film structure. An exact calculation of reflectivities requires allowance for refraction within the film, and can be achieved using methods developed from optics, where the film density profile is considered to be divided up into a finite number of slices. As in all scattering techniques, the scattering density distribution cannot be obtained directly. However, in the case of specular reflectivity the information content is further limited by the one-dimensional nature of the profile. Modelling is required to extract quantitative information.

1.10 COMPUTER SIMULATION

1.10.1 Monte Carlo Method

This involves simulating the thermodynamic properties of a box of particles, interacting through a potential specified by the programmer. As computers rapidly become more powerful, the number of particles that can be simulated in a Monte Carlo box increases. It is now possible to simulate millions of single particles. At each step, the particles are moved through small, random distances and the total potential energy change, ΔV, of the system is calculated. Whether this new configuration is accepted or not is then judged according to whether ΔV is less than or greater than that prior to the iteration step. This is termed the Metropolis sampling method, which is the simplest type of Monte Carlo simulation. If $\Delta V < 0$, then the new configuration is accepted. If $\Delta V > 0$, then the new configuration can be accepted or rejected. The probability of acceptance is proportional to the Boltzmann factor, $\exp(-\Delta V/k_{\mathrm{B}}T)$. This ensures that, at equilibrium, the particles are partioned among potential energy levels according to a Boltzmann distribution. The system is considered to reach equilibrium when the potential energy of the system is constant over repeated further steps. Usually many thousands or millions of cycles are necessary to achieve equilibrium. When equilibrium is reached, statistical thermodynamic quantities such as pair distribution functions can be computed by averaging over a series of cycles. Although Monte Carlo methods involve moving particles, there is no attempt to realistically model their dynamics because they are just moved randomly by a small amount at each time step. However, it does simulate configurations of molecules from which equilibrium thermodynamic and structural properties can be computed.

To conserve the number of particles in the simulation box and to prevent the boundaries of the box having any effect on the properties of the system, periodic boundary conditions are applied. This means that if a particle leaves the box through one face by moving a given distance, an identical particle is moved in by the same distance from a periodic image of the box (Fig. 1.11). Periodic boundary conditions are applied in all computer simulation

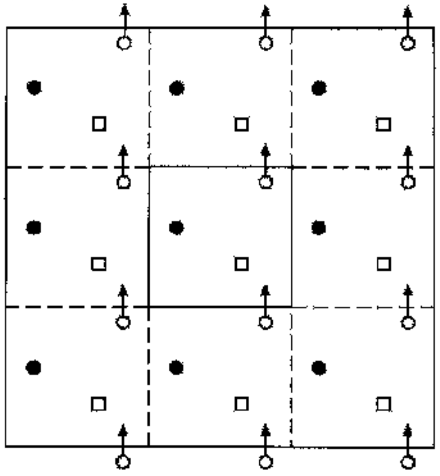

Figure 1.11 Periodic boundary conditions in a computer simulation. A particle that leaves the top of the simulation box (centre) is replaced by an identical one, moving by the same amount out of a periodic image of the original box

methods where particles are moved in a box, including molecular dynamics and Brownian dynamics as well as Monte Carlo simulations.

1.10.2 Molecular Dynamics Method

Here, the movements of molecules are simulated by assuming that they obey Newton's laws of motion. This provides a reasonable model for molecular dynamics over short time-scales. Starting from an initial configuration, the trajectories of all the particles interacting under the influence of specified intermolecular potentials are followed. Newton's laws of motion are used to compute the position of each particle after a short time step, which corresponds to about 10^{-15} s, when comparison is made with the time-scale of real molecular motions. When equilibrium is reached, the total potential energy is constant for subsequent iterations. Then equilibrium quantities such as pair distribution functions can be calculated, since the positions of all particles are known. Reliable values are usually obtained by averaging over many cycles. Thermodynamic quantities such as internal energy can then be computed from the pair distribution function. A major problem encountered in molecular dynamics equations is that numerical integration of the equations can lead to small numerical errors. These can build up over many time steps and lead to changes in the kinetic energy, and hence to the average temperature of the system. These temperature drifts (which can be upwards or downwards) are corrected by occasional rescaling of the particle velocities.

In contrast to Monte Carlo simulations, the molecular dynamics method simulates the motions of molecules; however, this can only be extended up to very short time-scales because the time step per cycle is so small. Thus, the method cannot be used to model collective motions, which are important in diffusion and hydrodynamic flows, for example. For this it is necessary to turn to more coarse-grained models, where molecular details are ignored. Here the properties of collections of molecules are simulated, or the fluid structure is simulated at an even larger length-scale where the system behaves as a continuum. Some of these methods are now discussed.

1.10.3 Brownian Dynamics Method

As the name suggests, this method simulates the Brownian motion of macromolecular or colloidal particles due to random collisions with the surrounding molecules. The collisions are simulated by a random stochastic force, so that the medium is effectively treated as a viscous continuum within which the particles move. The continuum dissipates the kinetic energy imparted to the particles by the collisions. In consequence, the temperature does not drift from its value controlled by the mean square force, which is proportional to $k_B T$. Brownian dynamics simulations are useful where molecular dynamics methods are inappropriate, i.e. for processes with slow dynamics such as polymers under flow.

1.10.4 Mesoscopic Methods

The Lattice Boltzmann method involves simulating a Boltzmann distribution of velocities on each site of a lattice. The distribution functions are allowed to evolve on a lattice to an equilibrium chosen to satisfy given conservation laws. On sufficiently large length- and time-scales, the macroscopic hydrodynamic equations are obeyed. The method is thus suitable for modelling complex flows induced by shear, as well as diffusive processes such as phase separation.

The dissipative particle dynamics (DPD) method is a recent variation of the molecular dynamics technique. Here, in addition to Newtonian forces between hard particles, soft forces between particles are also introduced. These pairwise damping and noise forces model slower molecular motions. The dissipative forces also reduce the drift in kinetic energy that occurs in molecular dynamics simulations. These two reasons mean that DPD can be used to model longer time-scale processes, such as hydrodynamic flows or phase separation processes.

Cell dynamics simulations are based on the time dependence of an order parameter, $\psi(\mathbf{r})$ (Eq. 1.23), which varies continuously with coordinate $\mathbf{r}$. For example, this can be the concentration of one species in a binary blend. An equation is written for the time evolution of the order parameter, $d\psi/dt$, in terms of the gradient of a free energy that controls, for example, the tendency for local diffusional motions. The corresponding differential equation is solved on a lattice, i.e. the order parameter $\psi(\mathbf{r})$ is discretized on a lattice, taking a value ψ_i at lattice point i. This method is useful for modelling long time-scale dynamics such as those associated with phase separation processes.

FURTHER READING

Atkins P. W., *Physical Chemistry*, 8th Edition, Oxford University Press, Oxford (2006).
Ball, P. *Made to Measure*, Princeton University Press, Princeton (1997).

Banwell, C. N. and E. M. McCash, *Fundamentals of Molecular Spectroscopy*, 4th Edition, McGraw-Hill, London (1994).

Evans, D. F. and H. Wennerström, *The Colloidal Domain. Where Physics, Chemistry, Biology and Technology Meet*, 2nd Edition, Wiley–VCH, New York (1999).

Hunter, R. J., *Foundations of Colloid Science*, Vol. I, Oxford University Press, Oxford (1987).

Jönsson, B., B. Lindman, K. Holmberg and B. Kronberg, *Surfactants and Polymers in Aqueous Solution*, Wiley, Chichester (1998).

Larson, R. G., *The Structure and Rheology of Complex Fluids*, Oxford University Press, New York (1999).

Shaw, D. J., *Introduction to Colloid and Surface Chemistry*, 4th Edition, Butterworth–Heinemann, Oxford (1992).